



ELSEVIER

Journal of Alloys and Compounds 228 (1995) 122–126

Journal of
ALLOYS
AND COMPOUNDS

Synthesis and structure investigation of the new ternary boride $(\text{Cr}_{0.80}\text{W}_{0.20})_3\text{B}_4$ and its analogues $(\text{Cr}_{1-x}\text{TM}_x)_3\text{B}_4$ with $\text{TM} = \text{Mo}$ or Ta

Yang Yu, Torsten Lundström

Institute of Chemistry, Uppsala University, Box 531, S-751 21 Uppsala, Sweden

Received 13 April 1995

Abstract

Single crystals of $(\text{Cr}_{1-x}\text{M}_x)_3\text{B}_4$ ($\text{TM} = \text{W}, \text{Mo}$ or Ta) have been synthesized by the high temperature metal–solution method using aluminium flux. They all crystallize in the Ta_3B_4 -type structure, with the space group *Immm* (No. 71) and unit-cell dimensions $a = 3.033(1)$ Å, $b = 13.030(3)$ Å and $c = 2.9631(7)$ Å for $(\text{Cr}_{1-x}\text{Ta}_x)_3\text{B}_4$, $a = 3.0628(4)$ Å, $b = 13.140(1)$ Å and $c = 2.9783(3)$ Å for $(\text{Cr}_{1-x}\text{Mo}_x)_3\text{B}_4$ and $a = 3.0700(7)$ Å, $b = 13.193(3)$ Å and $c = 2.984(1)$ Å for $(\text{Cr}_{0.80}\text{W}_{0.20})_3\text{B}_4$. A single-crystal X-ray diffraction study was carried out on $(\text{Cr}_{1-x}\text{W}_x)_3\text{B}_4$ and a full-matrix least-squares crystal structure refinement was performed on the basis of the collected data. The refinement converged at an $R(F^2)$ value of 0.061 for 2151 reflections. In $(\text{Cr}_{1-x}\text{W}_x)_3\text{B}_4$ the tungsten and chromium atoms are randomly distributed, i.e. the same atomic ratio $([\text{W}]/[\text{Cr}] = 0.25)$ was found in the two 4g and 2c positions corresponding to $x = 0.20$ in the formula. The size of the TM atom situated at the 4g position has larger influence on the b value of the unit-cell dimensions than on the values of a and c . The solid solubilities of molybdenum and tungsten in Cr_3B_4 are discussed.

Keywords: Crystal synthesis; Crystal structure

1. Introduction

Several ternary borides have been reported to crystallize in the Ta_3B_4 -type structure [1–7]. In these ternary borides, the metal atoms occupy two different atomic positions, namely 4g and 2c (space group, *Immm*). The order of the metal atoms and the solid solubility of TM atoms in binary Ta_3B_4 -type compounds is of interest both for the crystal structure description and for the physical properties of these compounds. For example, Ishii et al. [6,7] have synthesized and studied the magnetic properties of $(\text{Mn}_{1-x}\text{TM}_x)_3\text{B}_4$ ($\text{TM} = \text{Cr}, \text{Ta}, \text{Mo}$ or W). They found that, in the range $0.1 \leq x \leq 0.4$, the TM atoms have preferentially occupied the 4g position. These phases were found to be ferromagnetic in the same compositional range and the Curie temperatures were found to change linearly with the volume of the unit cell for $\text{TM} = \text{Cr}, \text{Ta}$ or Mo .

In previous studies of ternary representatives of the Ta_3B_4 -type structure, the order of the metal atoms was investigated mainly by studying the compositional

dependence of the unit-cell parameters or the relationship between the magnetic properties and the compositional variation of these compounds. The early studies, however, did not present strong evidence for an order of the metal atoms in these ternary borides. In the present work, it was attempted to grow single crystals of ternary representatives of Ta_3B_4 in the Cr-TM-B systems ($\text{TM} = \text{W}, \text{Mo}$ or Ta) and to determine the order of the metal atoms in $(\text{Cr}_{1-x}\text{W}_x)_3\text{B}_4$ using single-crystal X-ray diffraction.

2. Experimental details

2.1. Crystal growth

Single-crystal growth of ternary $(\text{Cr}_{1-x}\text{TM}_x)_3\text{B}_4$ ($\text{TM} = \text{W}, \text{Mo}$ or Ta) was performed by the high-temperature metal solution method using aluminium flux [8,9]. The claimed purities of the starting materials were 99.998% (Highways International, Baarn, The

Netherlands), 99.95% (Koch-Light Laboratories, Colubrook, England), 99.6% (S.A. Lindberg & Co., Stockholm), 99.9% (Söderfors, Bruk, Sweden), 99.6% (H.C. Starck, Goslar, Germany) and 99.997% (Vigelands Bruk, Norway) for chromium, tantalum, molybdenum and tungsten metals, crystalline boron and aluminium, respectively. The initial atomic ratios for $[\text{Cr}]/[\text{TM}]$, $[\text{B}]/[\text{Cr} + \text{TM}]$ and $[\text{Al}]/[\text{Cr} + \text{TM}]$ were 3, 1.45 and 28 respectively.

The syntheses were performed in a vertical graphite furnace (Thermal Technology Inc. 1000-3560-FP-20) under the flow of pure argon gas (AGA, Sundbyberg, Sweden; claimed purity 99.998%). The mixture of the starting materials for each system was placed in an alumina crucible and was initially heated to 1650 °C, soaked at this temperature for 5 h, then cooled to 1000 °C at a cooling rate of 50 °C/h whereafter the furnace was switched off. The as-grown crystals were separated from the solidified excess aluminium in diluted hydrochloric acid (6 M).

2.2. X-ray and element analysis

X-ray powder diffraction patterns were recorded using a Guinier–Hägg camera with strictly monochromatic $\text{Cu K}\alpha_1$ radiation ($\lambda = 1.540598 \text{ \AA}$) and semiconductor-grade silicon ($a = 5.431065 \text{ \AA}$) as internal calibration standard [10]. The powder samples were obtained by crushing selected Ta_3B_4 -type crystals. The unit-cell parameters were determined by least-squares refinement using the local UNITCELL [11]. The unit-cell dimensions are listed in Table 1. An optical microscope and a Weissenberg X-ray camera were used to examine the as-grown crystals of the Ta_3B_4 type. The morphology of the ternary $(\text{Cr}_{1-x}\text{W}_x)_3\text{B}_4$ single crystals is shown in Fig. 1. Electron microprobe analysis of the above-mentioned crystals was performed in a scanning electron microscope (JEOL JSM-840) equipped with an energy-dispersive detector. The aluminium concentration was found to be below the limit of measurement for all these ternary compounds. Since tungsten has a larger scattering power for X-rays than the other TM elements in the present study, it is relatively easy to determine the atomic position and the occupancy

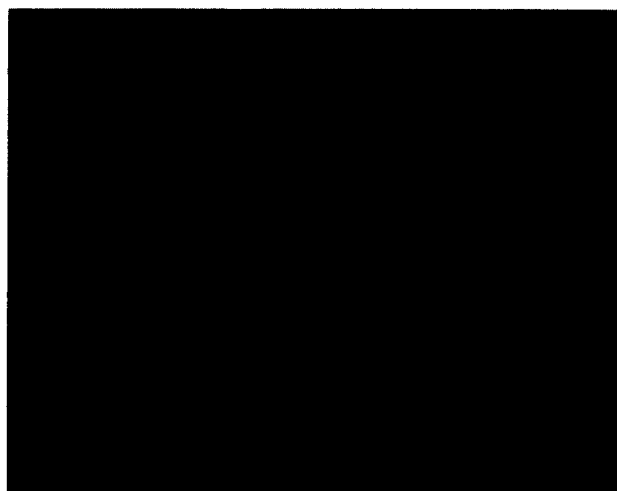


Fig. 1. A scanning electron micrograph of a $(\text{Cr}_{1-x}\text{W}_x)_3\text{B}_4$ single crystal. The two crystal surfaces which are parallel to the paper are $\{010\}$. The crystal is extending in the direction of $\{001\}$.

factor of the tungsten atom from X-ray diffraction data. Therefore a well-formed single crystal of $(\text{Cr}_{1-x}\text{W}_x)_3\text{B}_4$ with a suitable size was selected as a representative of these ternary borides $(\text{Cr}_{1-x}\text{TM}_x)_3\text{B}_4$ (TM = Ta, Mo or W), for single-crystal X-ray data collection and crystal structure refinement.

2.3. Intensity measurement

The X-ray intensities were measured with a Rigaku AFC6R automatic four-circle single-crystal diffractometer using graphite monochromated $\text{Mo K}\alpha$ radiation ($\lambda = 0.71069 \text{ \AA}$) and ω - 2θ scan technique. Six standard reflections were measured after each 150 reflections to check the stability of the primary X-ray beam and the equipment.

The collected intensity data were first corrected for Lorentz–polarization effects. A long-term systematic decrease in intensity was observed and consequently a linear decay correction was applied on the measured intensities. Since the tungsten compound has a very high absorption coefficient, the size of the $(\text{Cr}_{1-x}\text{W}_x)_3\text{B}_4$ single crystal was measured under a microscope and the shape of the crystal was properly described using the program SHAPE [14] for further

Table 1

Unit-cell dimensions of the binary and ternary representatives of the Ta_3B_4 in Cr–TM–B systems with TM = W, Mo and Ta (the estimated standard deviations are given in parentheses)

Phase	a (\AA)	b (\AA)	c (\AA)	V (\AA^3)	Reference
Cr_3B_4	3.0004(8)	13.018(3)	2.9516(8)	115.29	[12]
Ta_3B_4	3.29	14.0	3.13	144.2	[13]
$(\text{Cr}_{1-x}\text{W}_x)_3\text{B}_4$	3.0700(7)	13.193(3)	2.984(1)	120.86	This work
$(\text{Cr}_{1-x}\text{Mo}_x)_3\text{B}_4$	3.0628(4)	13.140(1)	2.9783(3)	119.86	This work
$(\text{Cr}_{1-x}\text{Ta}_x)_3\text{B}_4$	3.033(1)	13.030(3)	2.9631(7)	117.10	This work

absorption corrections. Absorption corrections were applied using the Gaussian grid technique. All these pre-refinement corrections of the original reflection data were carried out using the TEXSAN software system [15].

3. Refinement of $(\text{Cr}_{1-x}\text{W}_x)_3\text{B}_4$

The structure refinement of $(\text{Cr}_{1-x}\text{W}_x)_3\text{B}_4$ was carried out using the full-matrix least-squares program DUPALS [16]. The initial values for the atomic coordinates and displacement factors of $(\text{Cr}_{1-x}\text{W}_x)_3\text{B}_4$ were taken from the crystal structure parameters of the binary Cr_3B_4 [12]. Since there are two different atomic positions for the metal atoms in the Ta_3B_4 -type crystal structure, the tungsten atoms may be distributed according to three different schemes, namely at 4g site or at 2c site or at both sites. All the three possible situations were tested in the crystal structure refinements. For each situation, the positional parameters, the isotropic displacement parameters and the occupancy factor for the tungsten atom were constrained to the corresponding parameters of the chromium atom(s). It turned out that the third situation (tungsten atoms occupy both 4g and 2c sites) gave the best results in the refinement.

It was found that for the strongest reflections the observed intensities were systematically lower than the calculated values, which means that they suffered from extinction effects. Consequently, an extinction correction was applied in the refinement. Different types of extinction correction were tried and finally the type I isotropic extinction was found to give the best result in the refinement, which decreased the R value from 14% to 11%. The occupancy parameters for boron positions were also refined, but no significant deviation from full occupancy was obtained. The anisotropic displacement parameters were then refined for the chromium and boron atoms and constrained for the tungsten atom. Prior to the final refinement, all the structure parameters were fixed except for the positional and anisotropic displacement parameters of the tungsten atom. No significant difference was found for the positional parameter between tungsten and chromium atoms. For the anisotropic displacement parameters, however, differences were found between tungsten and chromium atoms, as shown later in Table 3.

The final refinement was based on F^2 , with a total of 19 refined parameters (one scale factor, three positional parameters, two occupancy parameters, 12 anisotropic displacement parameters and one isotropic extinction parameter), and nine constrained parameters (one positional parameter, two occupancy parameters and six anisotropic displacement parameters).

Table 2

Crystal data and refinement parameters of $(\text{Cr}_{0.80}\text{W}_{0.20})_3\text{B}_4$

Space group: Z	$Im\bar{3}m$; 4
Crystal dimensions (mm \times mm \times mm)	0.04 \times 0.05 \times 0.05
Cell parameters	
a (Å)	3.0700(7)
b (Å)	13.193(3)
c (Å)	2.984(1)
Refined formula	$(\text{Cr}_{0.80}\text{W}_{0.20})_3\text{B}_4$
Formula weight	278.34
Calculated density (g cm^{-3})	7.667
Absorption coefficient (cm^{-1})	392
Number of boundary planes	10
Transmission factor	0.118–0.261
2θ limit ($^\circ$)	124.2
Number of reflections	
Measured	2151
Observed ($>3\sigma$)	1563
Independent	673

For the final refinement, the C_1 and C_2 values [16] were 1.9 and 0.016 respectively. The S value (standard deviation of an observation of unit weight) [17] was 1.14, which indicated that the weights in the refinement are reasonable. Similarly, the analysis of the normal probability plot [17] of the ranked weighted differences gave a least-squares line slope of 1.00 and a y intercept of -0.05 , which indicates that a correct weighting scheme was used. Crystal and reflection collection data are listed in Table 2. The final structure data are presented in Table 3 and the interatomic distances in Table 4.

4. Results and discussion

Single crystals of $(\text{Cr}_{1-x}\text{TM}_x)_3\text{B}_4$ (TM = W, Mo or Ta) were obtained with the maximum size of 1 mm \times 0.4 mm \times 0.4 mm. Since the morphologies of these crystals are similar, only a $(\text{Cr}_{1-x}\text{W}_x)_3\text{B}_4$ single crystal is presented in scanning electron micrograph in Fig. 1.

The crystal structure of ternary $(\text{Cr}_{0.80}\text{W}_{0.20})_3\text{B}_4$ is illustrated in Fig. 2. It can be described as a kind of slab packing along the y axis in a similar manner as was used for the description of the V_2B_3 -type structure [18]. Each slab is composed of two layers of close-packed $\text{B}(\text{TM})_6$ trigonal prisms (TM = Cr or W). At $y = \frac{1}{2}$, the slab is displaced by the vector $\frac{1}{2}, 0, \frac{1}{2}$. Direct contacts between the TM atoms exist between each slab, forming rectangular TM pyramids. The prism axis is parallel to the x axis. Instead of boron triple chains in the V_2B_3 -type structure, there are double chains in the structure of $(\text{Cr}_{0.80}\text{W}_{0.20})_3\text{B}_4$. These boron zigzag chains extend in the z -axis direction on the y - z plane. Those metal atoms which are situated in between the boron double chains occupy the 4g positions. The other metal atoms, which are located above and below the boron double chains in the x axis direction, occupy

Table 3

Final structure data for $(\text{Cr}_{0.80}\text{W}_{0.20})_3\text{B}_4$, where the e.s.d.'s are given in parentheses; the displacement factor is described as $\exp\{-2\pi^2(U_{11}h^2a^{*2} + U_{22}k^2b^{*2} + U_{33}l^2c^{*2} + 2U_{12}hka^*b^* + 2U_{13}hla^*c^* + 2U_{23}klb^*c^*)\}$, where $U_{12} = U_{13} = U_{23} = 0$ and $U_{ii} \times 10^4$ (\AA) ($R = 0.061$ and $R_w = 0.07$, for all measured reflections) (space group, *Immm*)

Atom	Position	x	y	z	Occupancy	B_{eq} (\AA)	U_{11}	U_{22}	U_{33}
Cr(1)	4g	0	0.18650(2)	1	0.800(8)	0.404(6)	50.7(8)	46.0(7)	51.9(8)
W(1)	4g	0	0.18650(2)	0	0.200(8)	0.349(6)	50.1(8)	39.1(8)	43.5(8)
Cr(2)	2c	$\frac{1}{2}$	$\frac{1}{2}$	0	0.800(8)	0.44(1)	59(1)	52(1)	56(4)
W(2)	2c	$\frac{1}{2}$	$\frac{1}{2}$	0	0.200(8)	0.42(1)	58(1)	50(1)	53(1)
B(1)	4g	0	0.3618(2)	0	1	0.37(6)	58(8)	60(10)	23(7)
B(2)	4h	0	0.4336(2)	$\frac{1}{2}$	1	0.37(6)	48(8)	55(9)	39(8)

Table 4

Interatomic distances in $(\text{Cr}_{0.80}\text{W}_{0.20})_3\text{B}_4$. Distances listed are all TM–TM < 3.6 \AA , TM–B < 3.5 \AA and B–B < 3.2 \AA ; the estimated standard deviations are given in parentheses

Atoms	Distance (\AA)	Atoms	Distance (\AA)
TM(1)–4TM(1)	2.7184(4)	B(1)–2B(2)	1.768(2)
–2TM(1)	2.9840(6)	–2B(1)	2.9840(6)
–2TM(1)	3.0700(3)	–2B(2)	3.0703(3)
–2TM(2)	2.8775(5)	–2B(2)	3.085(4)
–4B(1)	2.2333(9)		
–2B(2)	2.206(2)	B(2)–B(2)	1.752(6)
		–2B(2)	2.984(6)
		–2B(2)	2.0700(3)
TM(2)–2TM(2)	2.9840(6)		
–2TM(2)	3.0700(3)		
–4B(1)	2.384(2)		
–8B(2)	2.313(1)		

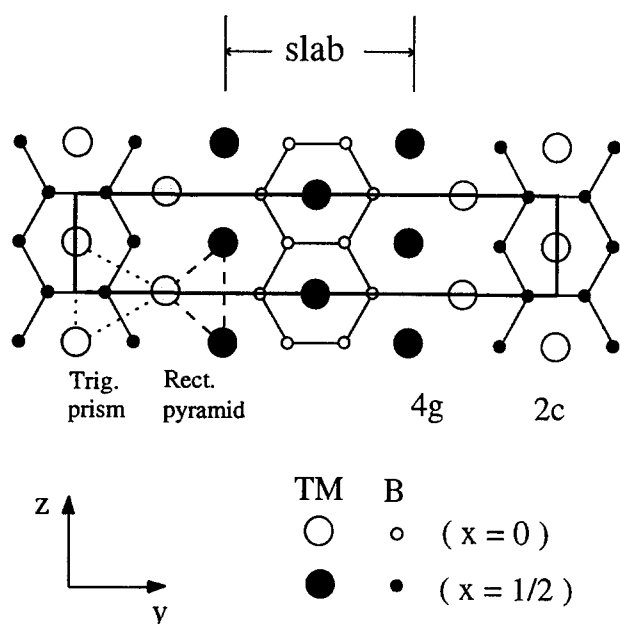


Fig. 2. The crystal structure of $(\text{Cr}_{0.80}\text{W}_{0.20})_3\text{B}_4$ projected in the xz axis direction. The projections of the unit cell, the slab, the trigonal prism, the rectangular pyramid along the same direction, the atomic positions of 4g and 2c are indicated.

the 2c positions. From the present single-crystal structure refinement of $(\text{Cr}_{0.80}\text{W}_{0.20})_3\text{B}_4$, it is evident that the tungsten and chromium atoms are accommodated at both 4g and 2c positions with the same $[\text{Cr}]/[\text{W}]$ ratio (equal to 4.0). Consequently, there is no order among the tungsten and chromium atoms in the ternary boride. The crystallographic support for this conclusion is very strong, since single-crystal diffraction was used (with a relative low final R value) and since there is a large difference between the atomic numbers of the metal atoms, which contributes to a high sensitivity in the determination of the occupancy factors.

The occurrence of several borides, which crystallize in the Ta_3B_4 -type structure, was reported earlier [1–7]. In some of these studies, an order of the metal atoms was claimed, but in no case was convincing evidence presented. However, since the two atomic positions accommodating the metal atoms are of different sizes, the explanation might be that the crystal studied was grown at such a high temperature that disorder was prevailing. At a lower temperature some order might occur, but from the growth condition it is not possible to determine at what temperature the crystal investigated actually was formed.

From Table 4, it can be seen that the shortest TM–TM distance is 2.718 \AA , which indicates that the TM atoms at the 4g positions have direct contacts and form rectangular pyramids between the slabs with the pyramid axes in the direction of the y axis. The interatomic distance between the TM atoms at 4g and 2c atomic positions is, however, 2.878 \AA , which is significantly more than twice the average atomic radius of tungsten (20%) and chromium (80%), 1.30 \AA . Similar to the situation in the V_2B_3 crystal structure [18], the B(1) atom in the $\text{B}(\text{TM})_6$ trigonal prism in the present structure is, in fact, not situated exactly at the centre of the prism. It is closer to the TM atoms at the 4g positions (2.233 \AA) than to the TM atoms at the 2c positions (2.384 \AA), which was discussed in detail in [18].

It is also interesting to note how the order of the metal atoms at different atomic positions (4g and 2c) influences the unit-cell parameters, especially the b

value. As mentioned above, the TM atoms at the 4g position have direct contacts with their neighbouring TM atoms along the y direction and form rectangular pyramids. If some of these TM atoms are replaced by other metal atoms with a larger atomic radius, the unit cell expands correspondingly in the y direction. The influence is not the same, however if some of the 2c positions accommodates other larger metal atoms, since the TM atoms at the 2c position do not have direct contact in the y direction with their neighbouring TM atoms. The space required to accommodate larger TM atoms at such positions is mainly determined by the size of the rigid boron double chains. Therefore the accommodation of larger metal atoms at the 4g position has a larger influence on the b value of the unit cell than the accommodation of the metal atoms at the 2c position.

The solid solubility of molybdenum in Cr_3B_4 was studied by Kuz'ma et al. [4]. From their investigation, 16 at.% Mo was found to dissolve in Cr_3B_4 . In the present investigation of the ternary systems of Cr–TM–B (TM = Mo, W or Ta), only the tungsten compound was studied by single-crystal diffractometry. However, some information about the solid solubilities of molybdenum and tantalum in Cr_3B_4 can be obtained by comparisons of the atomic radii of the TM elements and the unit cell dimensions of these ternary compounds. According to [19], the atomic radii (coordination number, 12) are 1.40 Å, 1.41 Å and 1.46 Å for molybdenum, tungsten and tantalum respectively. If tantalum has the same solid solubility in Cr_3B_4 as the other two, the unit-cell dimension of the ternary tantalum compound should be larger than those of the other two ternary compounds. From the present experiments, however, the unit-cell dimension of the ternary tantalum compound is considerably smaller than those of the other two, as shown in Table 1. In fact, it is not far from that of Cr_3B_4 . Consequently, the solid solubility of tantalum in Cr_3B_4 is significantly lower than those of molybdenum and tungsten, since the initial [Cr]/[TM] ratios in the flux were the same for all experiments. For the molybdenum and tungsten ternary compounds, the unit-cell volume of the former is about 0.8% smaller than that of the latter. In addition, the atomic radii of these two elements are very close; it is evident that the solid solubility of molybdenum in Cr_3B_4 [4] is slightly lower than that of tungsten (20 at.%, as seen in Table

2). This estimation is in good agreement with the experimental result reported by Kuz'ma et al. [4].

Acknowledgements

Financial support provided by the Swedish Nature Science Research Council is gratefully acknowledged. The authors are also indebted to Lars-Erik Terenius and Mr. Anders Lund for their assistance during the single-crystal growth. Thanks are also due to Mr. Hilding Karlsson for his help during the data collection.

References

- [1] Haschke, H. Nowotny and F. Benesovsky, *Monatsh. Chem.*, 97 (1966) 1459.
- [2] Yu. B. Kuz'ma, O.V. Nych and R.V. Skolozdra, *Inorg. Mater. (Engl. Transl.)* 2 (1966) 1709.
- [3] E.I. Gladyshevskij, T.F. Fedorov, Yu. B. Kuz'ma and R.V. Skolozdra, *Sov. Powder Metall. Met. Ceram.*, 4 (1966) 305.
- [4] Yu. B. Kuz'ma, V.S. Telegus and D.A. Kovalyk, *Porosh. Met.*, 9(5) (1969) 79.
- [5] P. Rogl, F. Benesovsky and H. Nowotny, *Monatsh. Chem.*, 103 (1972) 965.
- [6] T. Ishii, M. Shimada and M. Koizumi, *J. Chem. Phys.*, 78, Part 1 (1983) 3294.
- [7] T. Ishii, M. Shimada and M. Koizumi, *J. Chem. Phys.*, 79 (1983) 1511.
- [8] D. Elwell and H.J. Scheel, *Crystal Growth from High-Temperature Solutions*, Academic Press, London, 1975.
- [9] T. Lundström, *J. Less-Common Met.*, 100 (1984) 215.
- [10] R.D. Deslattes and A. Henins, *Phys. Rev. Lett.*, 31 (1973) 972.
- [11] B.I. Noläng, personal communication, Institute of Chemistry, Box 531, S-751 21 Uppsala, 1989.
- [12] S. Okada, T. Atoda and I. Higashi, *J. Solid State Chem.*, 68 (1987) 61.
- [13] R. Kiessling, *Acta Chem. Scand.*, 3 (1949) 603.
- [14] SHAPE: *Software for Drawing Crystals on Personal Computers*, 196 Beechwood Avenue, Bogota, NJ, 1988.
- [15] TEXSAN: *Single Crystal Structure Analysis Software, Version 5.0*, Molecular Structure Corporation, The Woodlands, TX, 1989.
- [16] J.-O. Lundgren (ed.), *Crystallographic Computer Programs, in UIC Publ. B18-4-5*, 1982 (Institute of Chemistry, Uppsala University).
- [17] J.A. Ibers and W.C. Hamilton (eds.), *International Tables for X-ray Crystallography*, Vol. IV, Kynoch, Birmingham, 1974.
- [18] Y. Yu, L.-E. Terenius, T. Lundström and S. Okada, *J. Alloys Comp.*, 221 (1995) 86.
- [19] F. Laves, *The Theory of Alloy Phases*, American Society for Metals, Cleveland, OH, 1956, p. 124.